# Ferrocenyl-dithiolane integrated Cu(I) Coordination Polymers: Framework Engineering for Synergistic Redox Activity towards Supercapattery Applications

Dilip Pandey[a], Mayank K. Singh[b], Sarvesh K. Maurya[a], Abhishek Ojha[a], Annika Schmidt[c], Carsten Strohmann[c], Lydie Viau[d]*, Michael Knorr[d]*, Dhirendra K. Rai[b]*, Abhinav Raghuvanshi[a]*

[a]*Department of Chemistry, Indian Institute of Technology Indore, Simrol, Indore, Madhya Pradesh, 453552, India.*

[b]*Sustainable Energy and Environmental Materials (SEEM) Lab, Department of Metallurgical Engineering and Material Science, Indian Institute of Technology Indore, Simrol, Indore, Madhya Pradesh, 453552, India.*

[c]*Anorganische Chemie, Technische Universität Dortmund, Otto-Hahn-Straße 6, 44227 Dortmund, Germany*

[d]*Université Marie et Louis Pasteur, CNRS, Institut UTINAM (UMR 6213), F-25000 Besançon, France*

**Email:** r.abhinav@iiti.ac.in *(AR)*

dkrai@iiti.ac.in *(DKR)*

lydie.viau@univ-fcomte.fr *(LV)*

michael.knorr@univ-fcomte.fr *(MK)*

**Table of contents**


1. General Information ……..…..…3

2. Experimental Section……..…5

Scheme S1. Synthesis of **L1**……..…6

Scheme S2. Synthesis of **L2**…….7

Figure S1. LCMS of **L1**……...……...…….....8

Figure S2. LCMS of **L2**……...…….....8

Figure S3. $^{1}$H NMR spectrum of **L1**……...……...…….....9

Figure S4.$^{13}$C{$^{1}$H} NMR spectrum of **L1**……...…….....9

Figure S5. $^{1}$H NMR spectrum of **L2**……..……....……..……10

Figure S6.$^{13}$C{$^{1}$H} NMR spectrum of **L2**……...…….....10

Figure S7. ORTEP plot of asymmetric unit of **L1**……..…….....11

Figure S8. ORTEP plot of asymmetric unit of **L2**……..…….....11

Figure S9. ORTEP plot of asymmetric unit of **Fc-Cu1**……..…….…...12

Figure S10. ORTEP plot of asymmetric unit of **Fc-Cu2**……..…….….12

Figure S11. Molecular structure of **L1**(a) and **L2**(b) **and** 2D structure of **Fc-Cu2 (c)**.....13

Table S1. Crystallographic parameters ……...……..……..…...14

Figure S12. IR spectra of **Fc-Cu1** and **Fc-Cu2** ……...……...…….....15

Figure S13. XPS survey of **Fc-Cu1** and **Fc-Cu2**.....…….……..….....15

Figure S14. Morphology of **Fc-Cu1** …….…….……..……..…..…….....16

Figure S15. Electrical conductivity of **Fc-Cu1** and **Fc-Cu2** ……..…….16

Figure S16. CV and GCD in negative and positive range of **Fc-Cu1** …….....17

Figure S17. CV and GCD in negative and positive range of **Fc-Cu2** ……. ……..….18

Figure S18. BET surface area analysis of **Fc-Cu1** and **Fc-Cu2**……. ……..……19

Figure S19. CV of **Fc-Cu1** at different scan rates……. ……..……19

Figure S20. GCD at different current densities of **Fc-Cu1**……. ……...…..…….20

Figure S21. Electrochemical kinetics analysis of **Fc-Cu1** and **Fc-Cu2** ……..…….....20

Figure S22. Comparison of PXRD patterns of **Fc-Cu2** …….……..…….....21

Figure S23. FE-SEM image of **Fc-Cu2** as synthesized, after cycling stability …...…… 21

Figure S24. Elemental mapping of **Fc-Cu2** after cycling stability……...…… 21

Table S2. Comparison table for efficiency in devices…...…….....22

Figure S25. DFT calculation……...……23
Table S3. Bader charge density analysis…...…….…….....24

# 1. General Information

## Materials and instrumentation

All the chemicals were used as received if not mentioned somewhere. All the chemicals used were purchased from Avra Chemicals and Acetonitrile (ACN), etc. were procured from Spectrochem and were directly used for synthesis. Mass spectra were obtained through the Bruker Daltonik High-Performance LCMS spectrometer. All the $^{1}H$ & $^{13}C\{^{1}H\}$ NMR spectra were obtained on Bruker 400 and 500 MHz spectrometer in $CDCl_3$. Chemical shifts are mentioned in delta (δ) units, shown in ppm downfield from tetramethyl silane (TMS) for $^{1}H$ NMR. $CDCl_3$ is used as an internal standard, which shows a peak at 7.26 ppm. The $^{1}H$ NMR splitting patterns have been mentioned as singlet(s), double(d), triplet(t) & multiplet(m). NMR data was processed by Mestre Nova. Powder X-ray diffraction (PXRD) data was recorded at 298 K on a Rigaku Smart X-ray diffractometer with monochromatic Cu Kα (0.1540 nm) radiation in $2\theta$ range of 5-50°. Bruker Alpha II spectrophotometer was used for FT-IR and Keithley model 6517B electrometer for conductivity experiments. The thermogravimetric analysis was performed on Mettler Toledo TGA/DSC 1 star e-system in the temperature range of 30-1000 °C. The electrical conductivity values of the two synthesized CPs have been recorded using the two-probe direct current method at 300 K on pressed pellets (5.0 GPa, 5 min). To perform the experiment, a Keithley model 6517B electrometer voltage source was used and silver paste was applied to contact the pressed pellets. The conductivity values of all the CPs were obtained by applying voltages ranging from −10 V to +10 V.

Suitable crystals of compounds **L1**, **L2**, **Fe-Cu1** and **Fe-Cu2** were mounted on a *MicroMount* from *MiTeGen* in combination with a *SMZ1279* stereomicroscope from *Nikon Metrology GmbH*.

For **L1:** Single crystal structure determination was performed on an Oxford Diffraction Xcalibur S diffractometer using graphite-monochromated Mo-K$\alpha$ radiation ($\lambda$ = 0.71073 Å). Data collection and reduction was performed using the CrysAlisPro software system (Version 1.171.33.55).[1] A multi-scan absorption correction using the CrysAlis RED program was employed.

For **L2:** Single-crystal measurements of **L2** were conducted using a suitable crystal on a SuperNova diffractometer. The diffraction data were collected at ambient temperature at 298 K utilizing Mo Kα radiation that was monochromatized with graphite (λ = 0.7107 Å) at 50 kV and 30 mA.

For **Fc-Cu1** and **Fc-Cu2**: Crystal structure determination was accomplished on a *Bruker D8 Venture* four-circle diffractometer using a *PHOTON II CPAD* detector by *Bruker AXS GmbH*. X-ray radiation was generated by microfocus source IμS Mo (λ = 0.71073 Å) by *Incoatec GmbH* with HELIOS mirror optics and a single hole collimator by *Bruker AXS GmbH*. For the data collection, the programs APEX 3 Suite (v.2018.7-2)[2], APEX 4 Suite (v2021.10-0)[3] and APEX 5 Suite (v2023.9-2)[4] with the integrated programs SAINT (integration) and SADABS (adsorption correction) by *Bruker AXS GmbH* were used.

The processing and finalization of the crystal structures was done with the program Olex2.[5] The crystal structure was solved with the ShelXT[6] structure solution program using Intrinsic Phasing and refined with the ShelXL refinement package using Least Squares minimization.[7] The non-hydrogen atoms were refined anisotropically. $U_{eq}$ is defined as one third of the trace of the orthogonalized tensor $U_{ij}$. For the hydrogen atoms the standard values of the SHELXL program were used with $U_{iso}(H) = -1.2\ U_{eq}(C)$ for $CH_2$ and CH and with $U_{iso}(H) = -1.5\ U_{eq}(C)$ for $CH_3$. An anharmonic refinement of the Cu and I atoms of compound **Fc-Cu2** with olex2.refine was conducted.

Field emission scanning electron microscopy (FESEM) images were taken on Carl Zeiss Supra 55 instruments after Au coating. Transmission Electron Microscope (TEM) images were taken from the electron microscope of model JEM-2100 at an accelerating voltage of 200 kV.

All calculations were performed using the Vienna Ab Initio Simulation Package (VASP) within a plane-wave framework. The interaction between core and valence electrons was treated using the projector augmented-wave (PAW) method together with the Perdew–Burke–Ernzerhof (PBE) exchange–correlation functional. A plane-wave energy cutoff of 550 eV was chosen to ensure reliable results, and spin polarization was included throughout. The structures were fully optimized until the total energy converged to $10^{-6}$ eV and the forces on each atom were below 0.03 eV $Å^{-1}$. Sampling of the Brillouin zone was performed using a Monkhorst–Pack 4 × 1 × 1 k-point mesh, with both atomic positions and lattice parameters allowed to relax.

## 2. Experimental Section

### Electrode Fabrication for Electrochemical Analysis

Initially, slurries were prepared using ultrasonication to disperse 10 mg of electrode materials in 1 mL of ethanol for 2 hours. At the same time, sections of carbon paper (CP) measuring 2x1 $cm^2$ were cut and thoroughly cleaned for subsequent use. Subsequently, the as-prepared slurry was drop-cast onto 1x1 cm of carbon paper (actual mass loading (mg $cm^{-2}$): **Fc-Cu1** (1.7 mg) and **Fc-Cu2** (1.9 mg)) and dried under vacuum for 4 hours. For all electrochemical tests, a 1 M potassium hydroxide (KOH) electrolyte solution was used.

### Electrochemical studies

**Charge storage study**: Electrochemical studies were performed using a NOVA software-controlled Autolab PGSTAT 204N. The reference electrode employed was Ag/AgCl, the counter electrode was made of platinum, and the working electrode consisted of carbon paper coated with the electrode material. The experiments included cyclic voltammetry (CV) at various scan rates and galvanostatic charge/discharge (GCD) at different current densities using an electrochemical workstation. Electrochemical impedance spectroscopy (EIS) was also carried out with a 10 mV AC amplitude over a frequency range spanning from 10 mHz to 100 kHz. The following equation was used to determine the specific capacity (C) using the GCD discharge curve.

$$C = \frac{I\,\Delta t}{m} \qquad (1)$$

where I is the current (A), $\Delta t$ is the discharge time (s), and m is the mass of the coated active material (g).

### Fabrication of symmetrical solid-state device:

A Swagelok cell having a 16 mm diameter was utilized for fabricating a solid-state symmetrical charge storage device. An electrode slurry was synthesized by subjecting 10 mg of electrode materials to sonication in a 1 mL ethanol solution for a period of 2 h. This resulting slurry was then dropcasted to a circular stainless steel mesh substrate and subsequently placed in an oven at 60 °C for 8 h to ensure proper drying. The electrolyte solution was prepared in 1g of PVA in 10 mL water. This mixture was then heated at 90 °C with continuous stirring for 3 h, to which 10 mL of a 1M KOH solution was added. Following this step, cellulose paper as a separator

was soaked into the resulting PVA-KOH gel electrolyte. Subsequently, the separator was sandwiched by two electrode material-coated stainless steel and assembled in a coin cell to fabricate a symmetrical supercapacitor device.

From the GCD curves, the following equations were used to derive the specific capacity, energy density (E), and power density (P) of the fabricated device.

$$C = \frac{I\,\Delta t}{m} \qquad (2)$$

$$E\left(\frac{Wh}{kg}\right) = \frac{0.5 \times C\Delta V}{3.6} \qquad (3)$$

$$P\left(\frac{W}{kg}\right) = \frac{3600 \times E}{\Delta t} \qquad (4)$$

Where m is the active material mass of both electrodes (g), Δt is the discharge time (s),I is the current (A), ΔV is the potential window (V), and C is the specific capacity of the device (C $g^{-1}$).

**Synthesis of L1:**

In a 50 mL round bottom flask, acetyl ferrocene (228 mg, 1 mmol) was dissolved in dichloromethane (1-2 mL) after that concentrated HCl (1 mL) and 1,2-ethanedithiol (103mg, 1.1 mmol) was added in the above reaction mixture. This reaction mixture was stirred for 6h at room temperature and the resulting product was extracted with dichloromethane and water mixture. The organic phase was washed several times with water, dried over anhydrous $Na_2SO_4$, and filtered. The solvent was evaporated under vacuum and the crude was purified by column chromatography [$C_6H_{14}$:EtOAc—97:3]. **L1** was obtained as a yellow solid which was recrystallized from a toluene/hexane mixtureYield: 237 mg, 78%, mp 115-116 °C. **$^1$H NMR** (500 MHz, $CDCl_3$) δ 4.36 (t, *J* = 1.8 Hz, 2H), 4.22 (s, 5H), 4.20 (t, *J* = 1.8 Hz, 2H), 3.52 – 3.37 (m, 4H), 2.21 (s, 3H). **$^{13}$C{$^1$H} NMR** (126 MHz, $CDCl_3$) δ (ppm): δ 95.4, 69.2, 68.5, 67.1, 65.3, 41.1, 33.9.

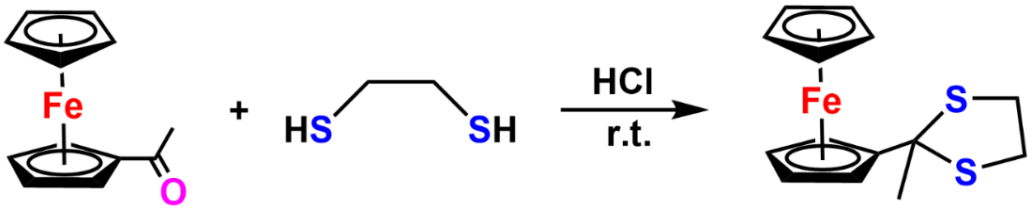


**Scheme S1:** Synthesis of **L1.**

**Synthesis of L2:**

In a 50 mL round-bottom flask, diacetyl ferrocene (270 mg, 1 mmol) was dissolved in dichloromethane (1-2 mL) after that concentrated HCl (1 mL) and 1,2-ethanedithiol (180 mg, 2.1 mmol) were added in the above reaction mixture. This reaction mixture was stirred for 6h at room temperature and the resulting product was extracted with dichloromethane and water mixture. The organic phase was washed several times with water, dried over anhydrous $Na_2SO_4$, and filtered. The solvent was evaporated under vacuum and the crude was purified by column chromatography [$C_6H_{14}$: EtOAc—98: 2]. The yellow solid product was obtained which was recrystallized from a toluene/hexane mixture. Yield: 337 mg, 80%, mp 120-121°C. **L2: $^1$H NMR** (400 MHz, $CDCl_3$) δ ppm): 4.38 (s, 4H), 4.28 (s, 4H), 3.62 – 3.00 (m, 8H), 2.21 (s, 6H). **$^{13}$C{$^1$H} NMR** (101 MHz, $CDCl_3$): δ (ppm) 95.7, 70.1, 67.5, 64.9, 40.8, 33.7.

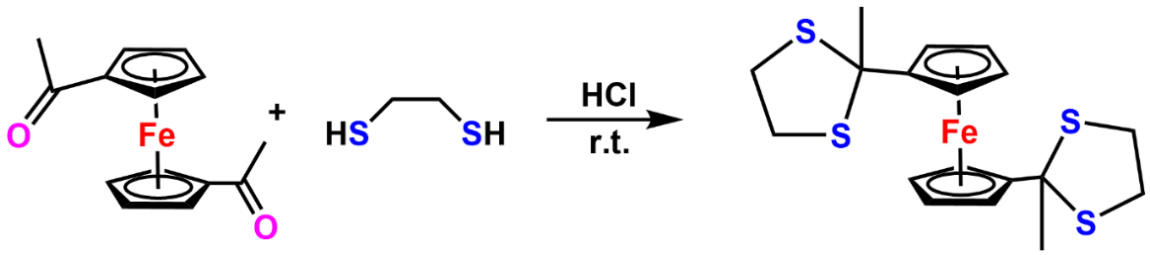


**Scheme S2:** Synthesis of **L2**

**Synthesis of Fc-Cu1 and Fc-Cu2:**

**Fc-Cu1:**

To a solution of CuI (0.08 mmol) in acetonitrile (3 mL) was added **L1** (0.04 mmol). The mixture was first stirred for 5 minutes at room temperature and then refluxed for 2 hrs into a pressure tube. The solution was then allowed to cool slowly to room temperature. The precipitate was filtered off and washed with dichloromethane and acetonitrile thrice to obtain yellow product in 76% (28 mg) yield. Anal. Calc for $C_{14}H_{16}Cu_2FeI_2S_2$ (685.12): %C 24.54, %H 2.35, %S 9.36, found: %C 24.41, %H 2.36, %S 9.20. IR (ATR): 3083, 2926, 2248, 1633, 1407, 1235, 1067, 831, 706, and 495 $cm^{-1}$.

**Fc-Cu2:**

To a solution of CuI (0.16 mmol) in acetonitrile (3 mL) was added **L2** (0.04 mmol). The mixture was first stirred for 5 minutes at room temperature and then refluxed for 2 hrs into a pressure tube. The solution was then allowed to cool slowly to room temperature. The precipitate was filtered off and washed with dichloromethane and acetonitrile thrice to obtain yellow product

in 80% (36 mg) yield. Anal. Calc for $C_{18}H_{22}Cu_4FeI_4S_4$ (1184.20): %C 18.26, %H 1.87, %S 10.83, found: %C 18.10, %H 1.92, %S 10.80. IR (ATR): 3081, 2918, 2329, 1616, 1395, 1228, 1022, 828, 696, and 482 $cm^{-1}$

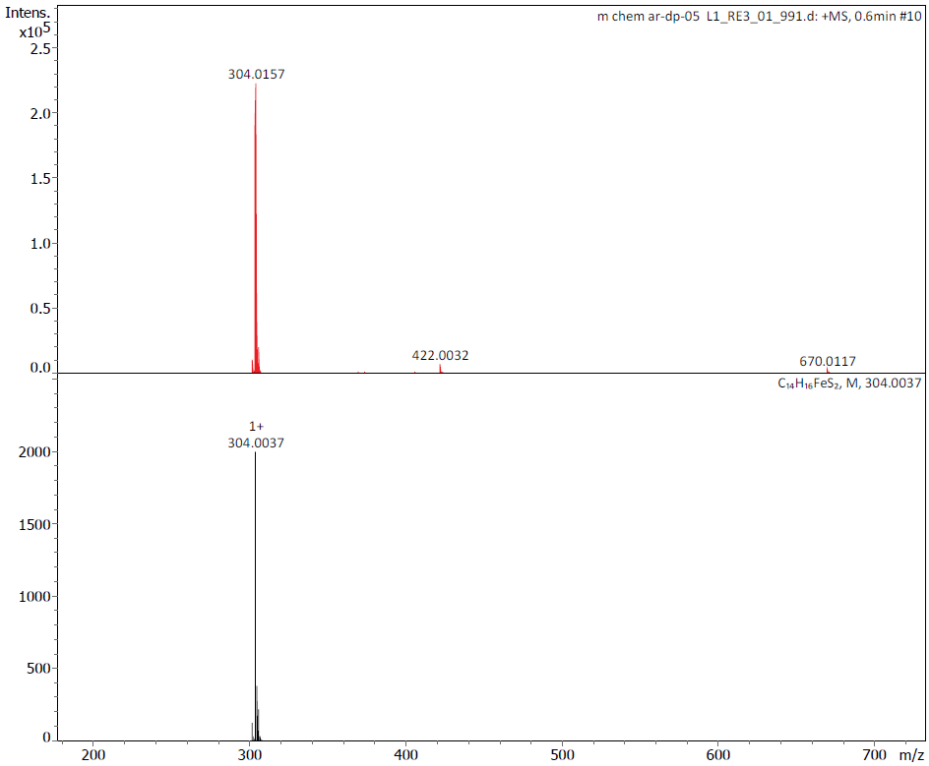


**Figure S1**. LCMS of **L1**

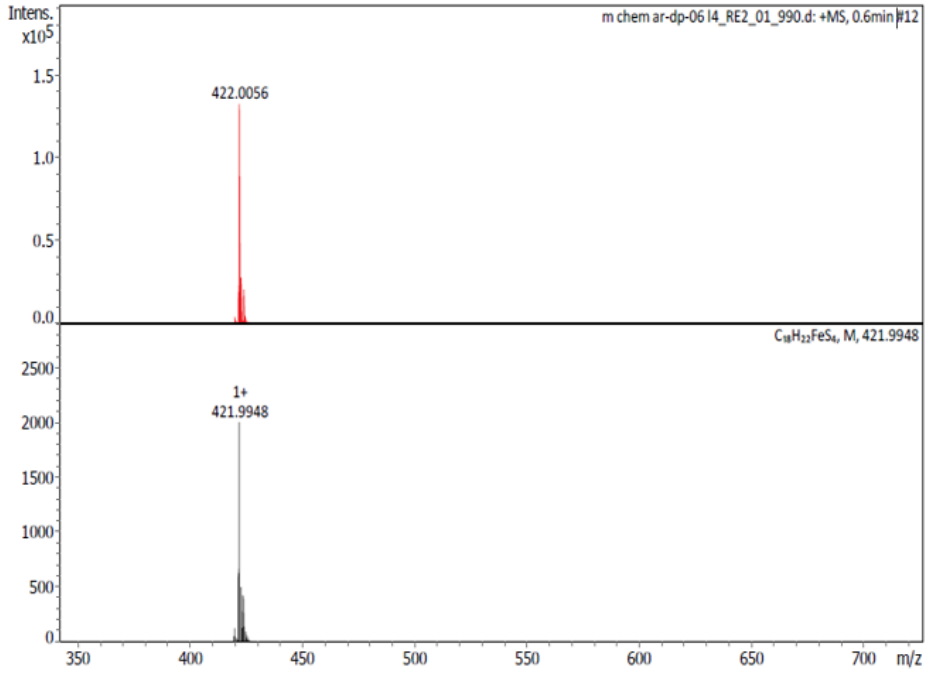


**Figure S2.** LCMS of **L2**

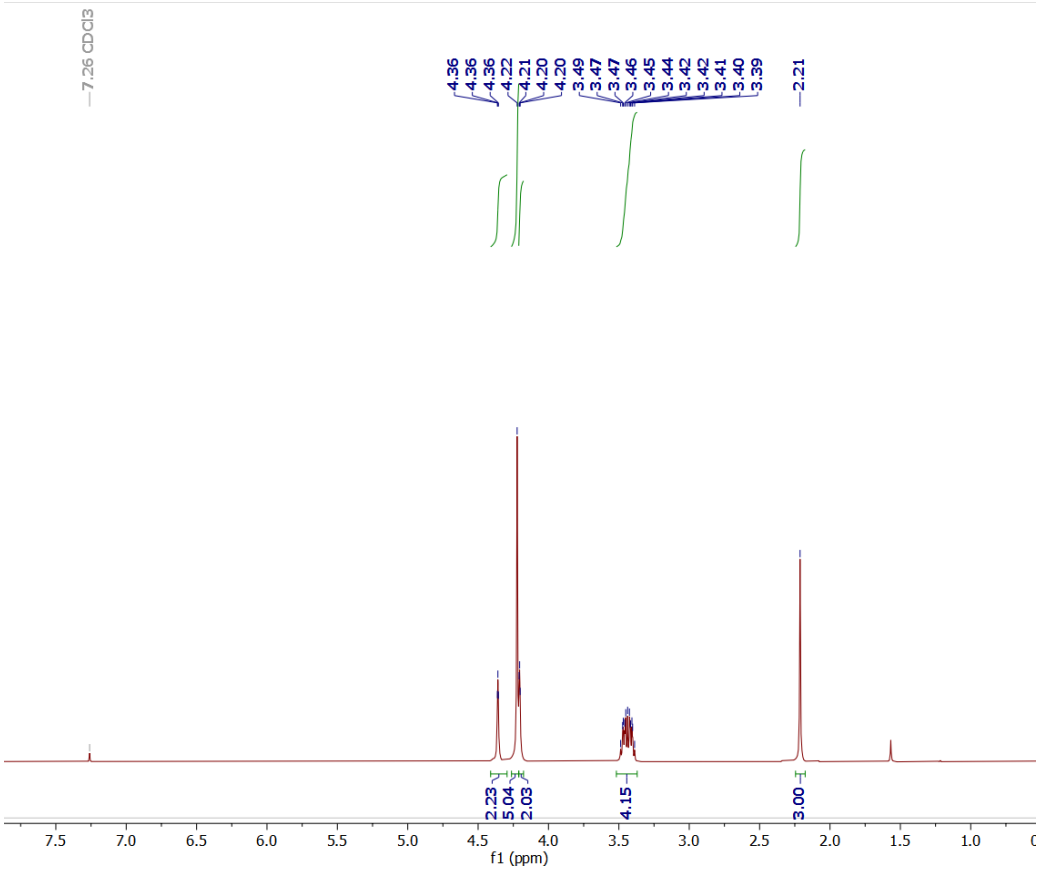


**Figure S3**. $^{1}H$ NMR spectrum of **L1**

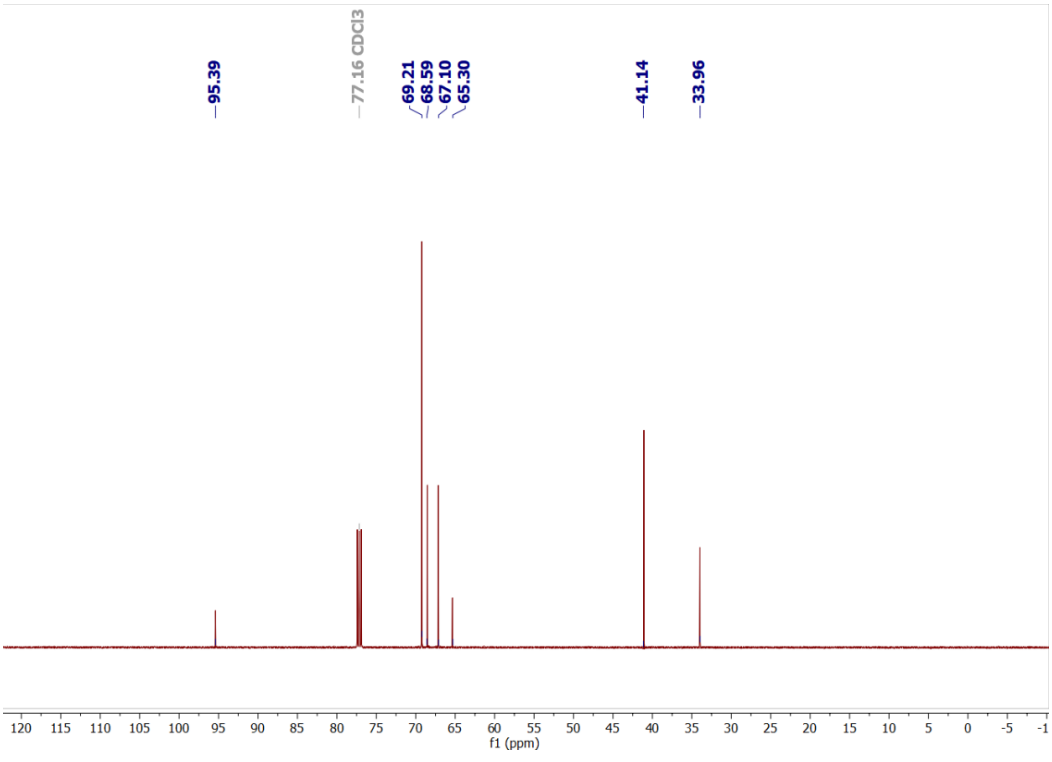


**Figure S4**. $^{13}C\{^{1}H\}$ NMR spectrum of **L1**

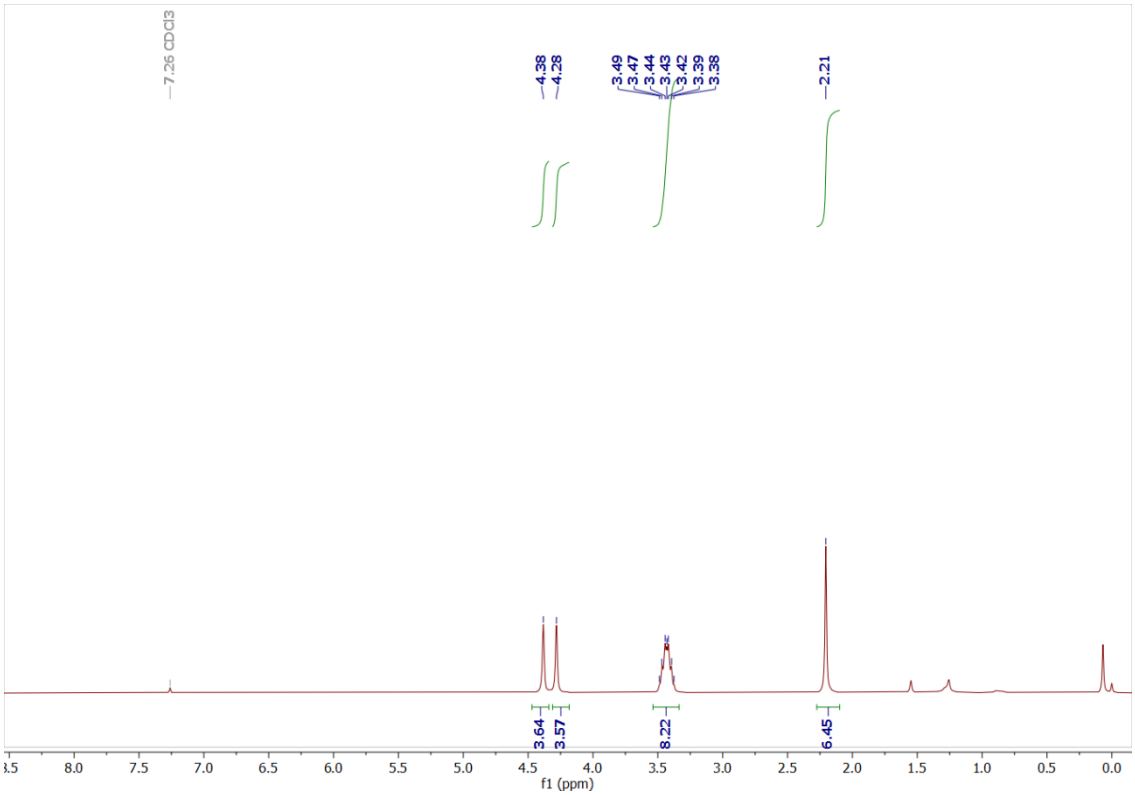


**Figure S5**. $^{1}$H NMR spectrum of **L2**

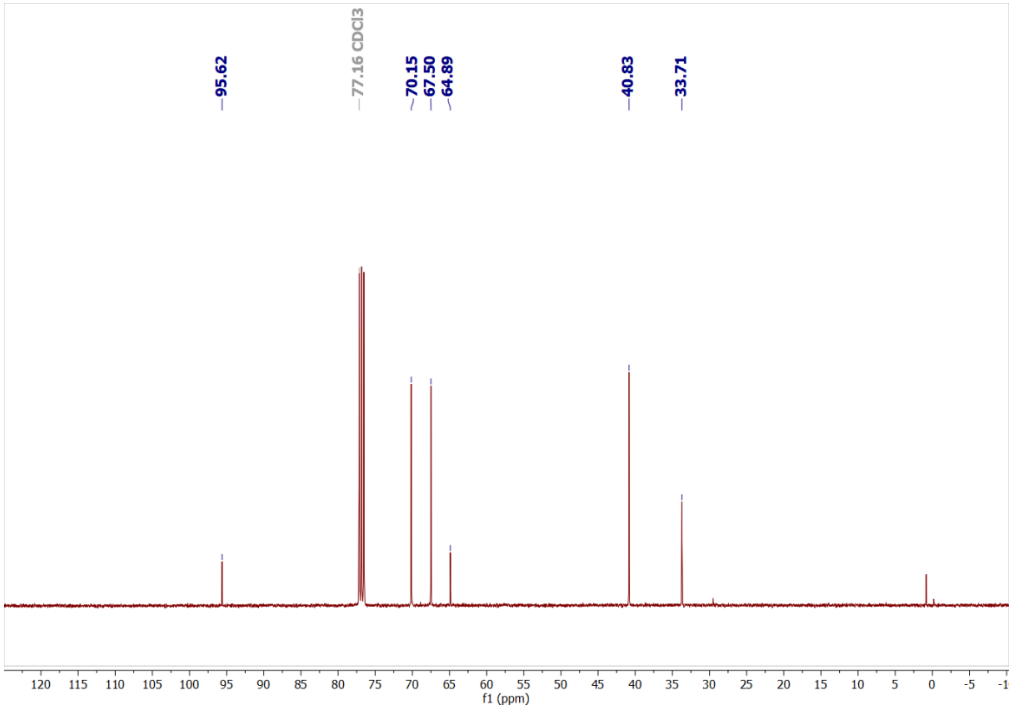


**Figure S6**. $^{13}$C{$^{1}$H} NMR spectrum of **L2**

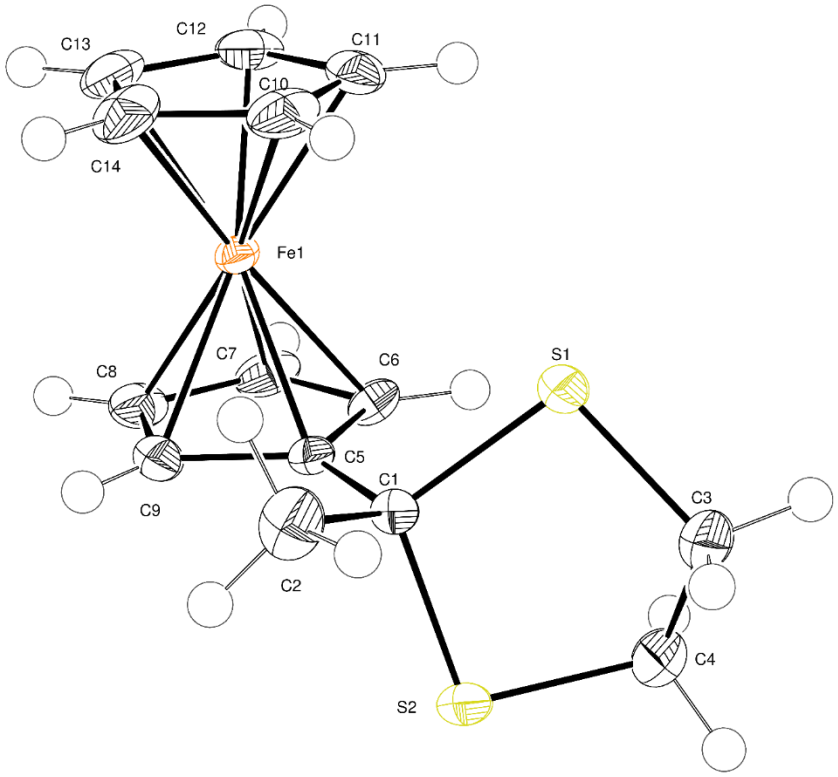


**Figure S7.** ORTEP plot of the asymmetric unit of **L1**. Elipsoid probability drawn at 70%.

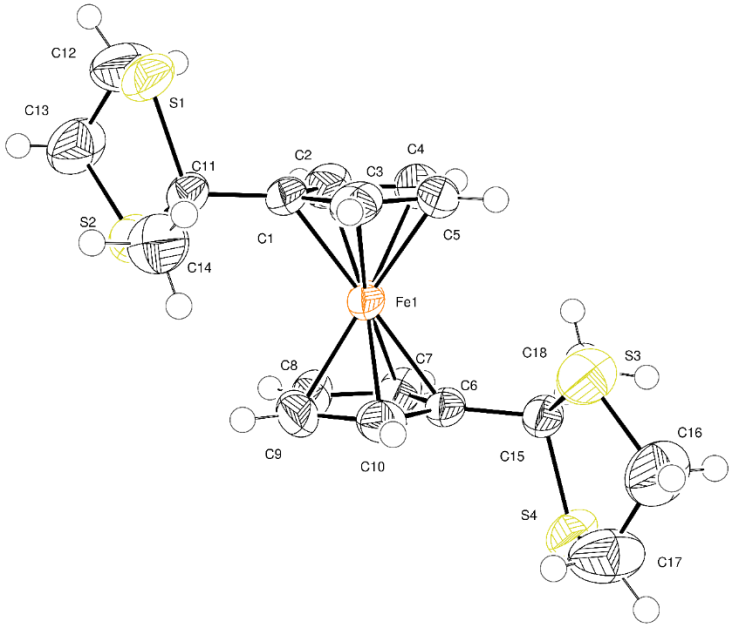


**Figure S8.** ORTEP plot of asymmetric unit of **L2**. Elipsoid probability drawn at 70%.

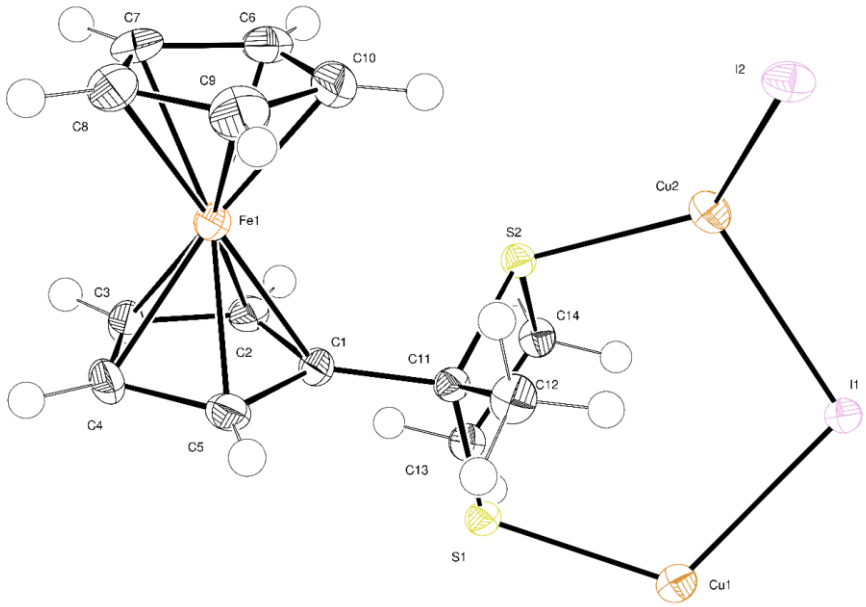


**Figure S9.** ORTEP plot of asymmetric unit of **Fc-Cu1**. Elipsoid probability drawn at 70%.

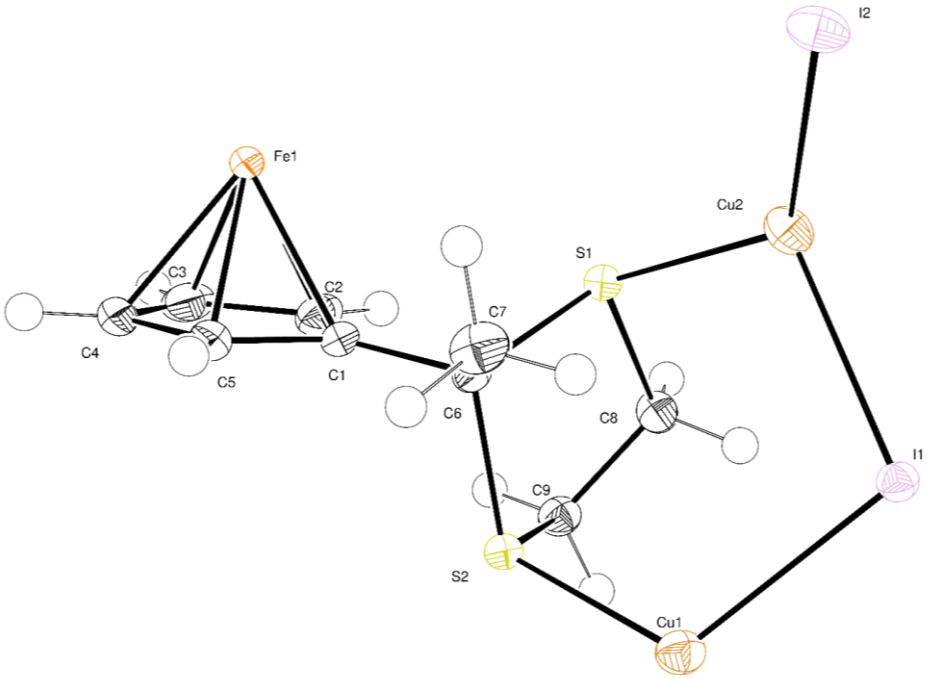


**Figure S10.** ORTEP plot of asymmetric unit of **Fc-Cu2**. Elipsoid probability drawn at 70%.

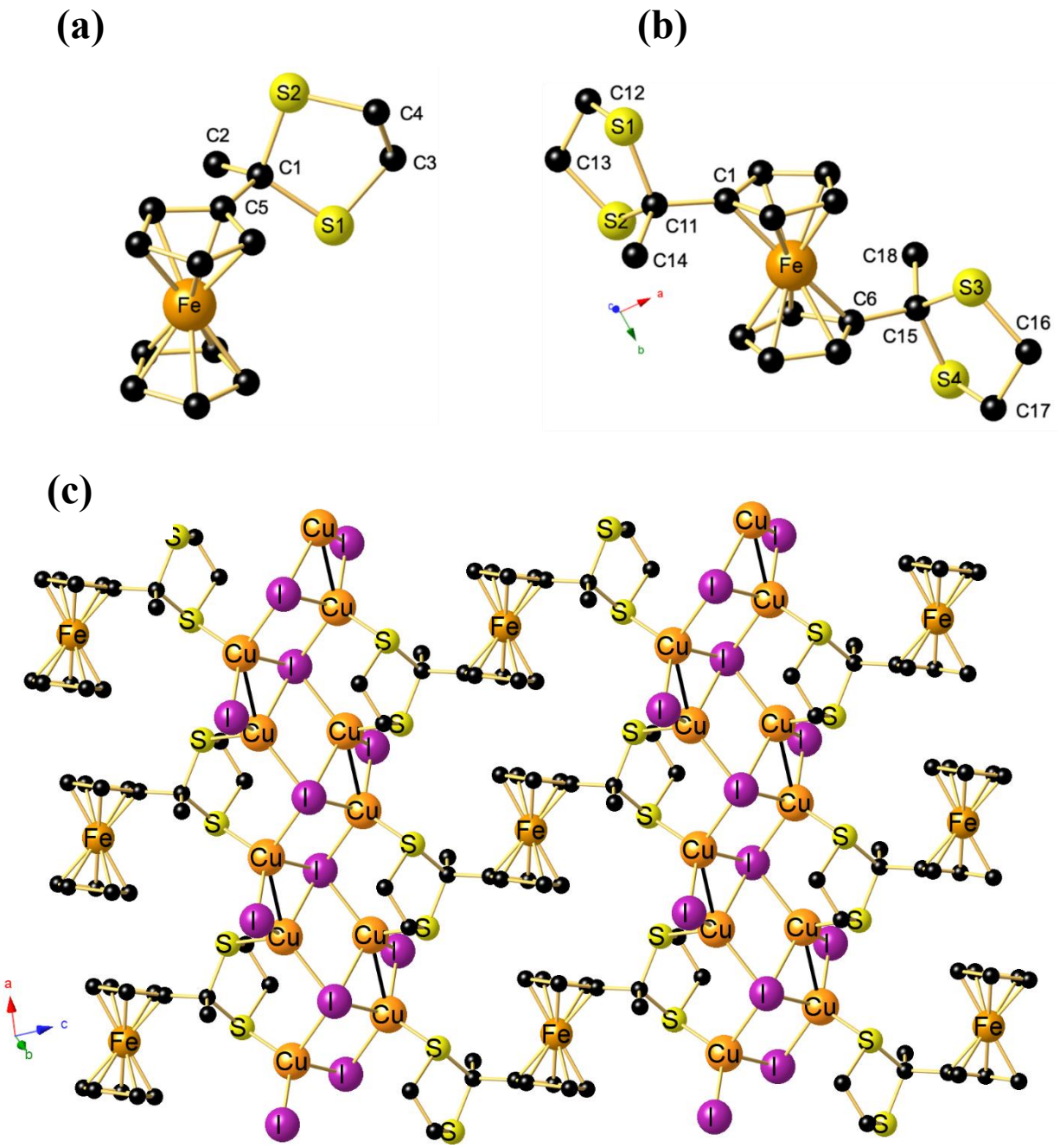


**Figure S11**. (a) Molecular structure of **L1**. (b) Molecular structure of **L2**. (c) 2D structure of **Fc-Cu2**

**Table S1:** Crystallographic parameters

| **Compound** | **L1** | **L2** | **Fc-Cu1**[1] | **Fc-Cu2** |
|---|---|---|---|---|
| **CCDC No** | **2417158** | **2417157** | **2417155** | **2417156** |
| **Formula** | $C_{14}H_{16}FeS_2$ | $C_{18}H_{22}FeS_4$ | $C_{14}H_{16}Cu_2FeI_2S_2$ | $C_{18}H_{22}Cu_4FeI_4S_4$ |
| **Formula weight** | 304.24 | 422.44 | 685.12 | 1184.20 |
| **Wavelength (Å)** | 0.71073 | 0.71073 | 0.71073 | 0.71073 |
| **Crystal system** | monoclinic | triclinic | triclinic | triclinic |
| **Space group** | *P2₁/n* | *P-1* | *P-1* | *P-1* |
| ***a*/Å** | 9.6132(4) | 8.2915(5) | 7.0071(7) | 7.0212(9) |
| ***b*/Å** | 6.4865(3) | 9.6749(8) | 7.3717(8) | 7.3853(6) |
| ***c*/Å** | 20.4989(8) | 11.5071(6) | 17.276(2) | 13.3339(9) |
| ***α*/°** | 90 | 88.030(5) | 86.632(4) | 99.823(3) |
| ***β*/°** | 90.323(4) | 87.689(4) | 83.531(4) | 91.654(6) |
| ***γ*/°** | 90 | 83.683(5) | 86.270(4) | 93.646(6) |
| **V/ Å$^3$** | 1278.21(9) | 916.33(11) | 883.63(17) | 679.34(11) |
| **Z** | 4 | 2 | 2 | 1 |
| **$\rho_{calcd}$ (g/cm$^3$)** | 1.581 | 1.531 | 2.575 | 2.895 |
| **Temperature/K** | 150.00 | 293.00 | 100.00 | 100.00 |
| **GOF** | 1.050 | 1.032 | 1.030 | 1.049 |
| **2*θ* range for data collection** | 6.588 to 59.438 | 5.978 to 49.998 | 4.752 to 60 | 5.612 to 69.994 |
| **Reflections collected** | 10048 | 9151 | 20389 | 143306 |
| **Independent reflections** | 3251 [$R_{int}$ = 0.0223] | 4308 [$R_{int}$ = 0.0327] | 5113 [$R_{int}$ = 0.0277] | 5979 [$R_{int}$ = 0.0429] |
| **Completeness to θ = 25.242** | 99.3 | 99.7 | 99.8 | 100 |
| **Final *R* indices [ I>2*σ*(I)]** | $R_1$ = 0.0240, w$R_2$ = 0.0591 | $R_1$ = 0.0397, w$R_2$ = 0.1021 | $R_1$ = 0.0268, w$R_2$ =0.0672 | $R_1$=0.0146, w$R_2$ = 0.0343 |
| **Final *R* indices [all data]** | $R_1$ = 0.0273, w$R_2$ = 0.0607 | $R_1$ = 0.0442, w$R_2$ = 0.1063 | $R_1$= 0.0314, w$R_2$ = 0.0704 | $R_1$ = 0.0163, w$R_2$ = 0.0350 |
| **Largest diff. peak/hole/ eÅ$^{-3}$** | 0.34/-0.30 | 0.60/-0.60 | 1.08/-0.96 | 1.15/-0.97 |

**[1] twin law applied (1, 0, 0, 0.143, -1, 0, 0.571, 0, -1) with BASF [0.1405(19)].**

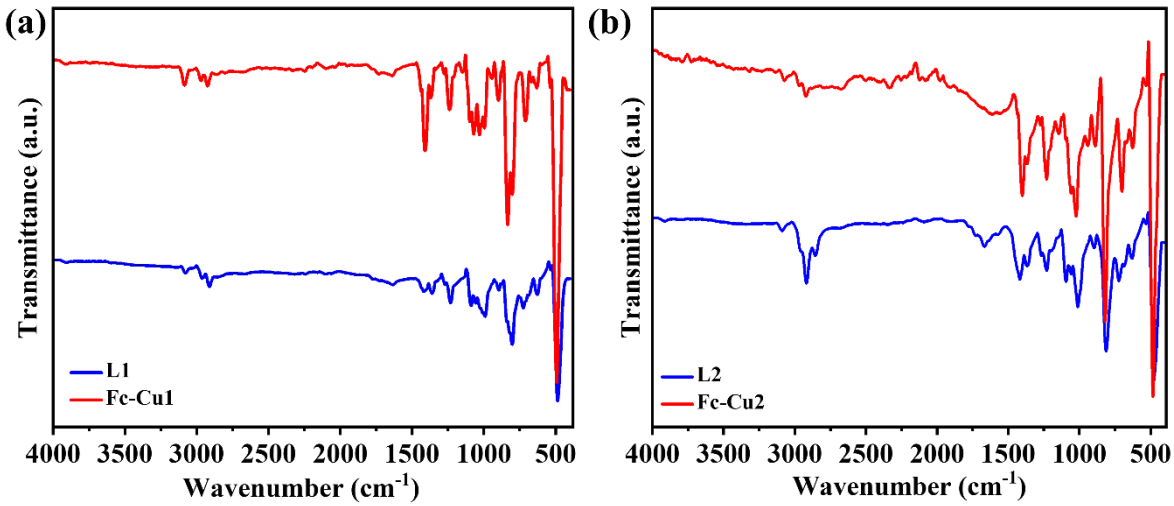


**Figure S12**. Comparison of IR spectra of (a) **Fc-Cu1** and **L1** (b) **Fc-Cu2** and **L2**

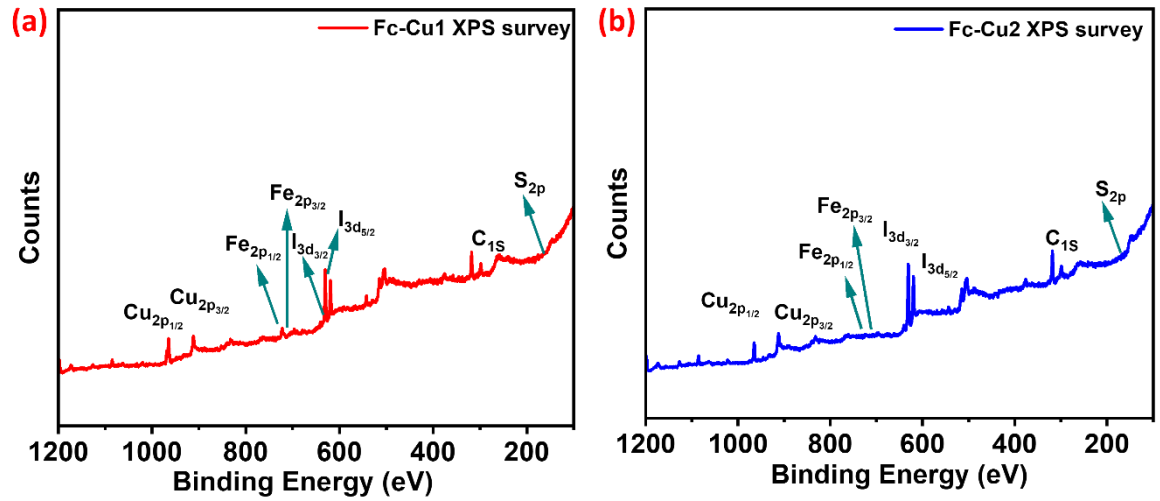


**Figure S13**. XPS survey of (a) **Fc-Cu1** (b) **Fc-Cu2**

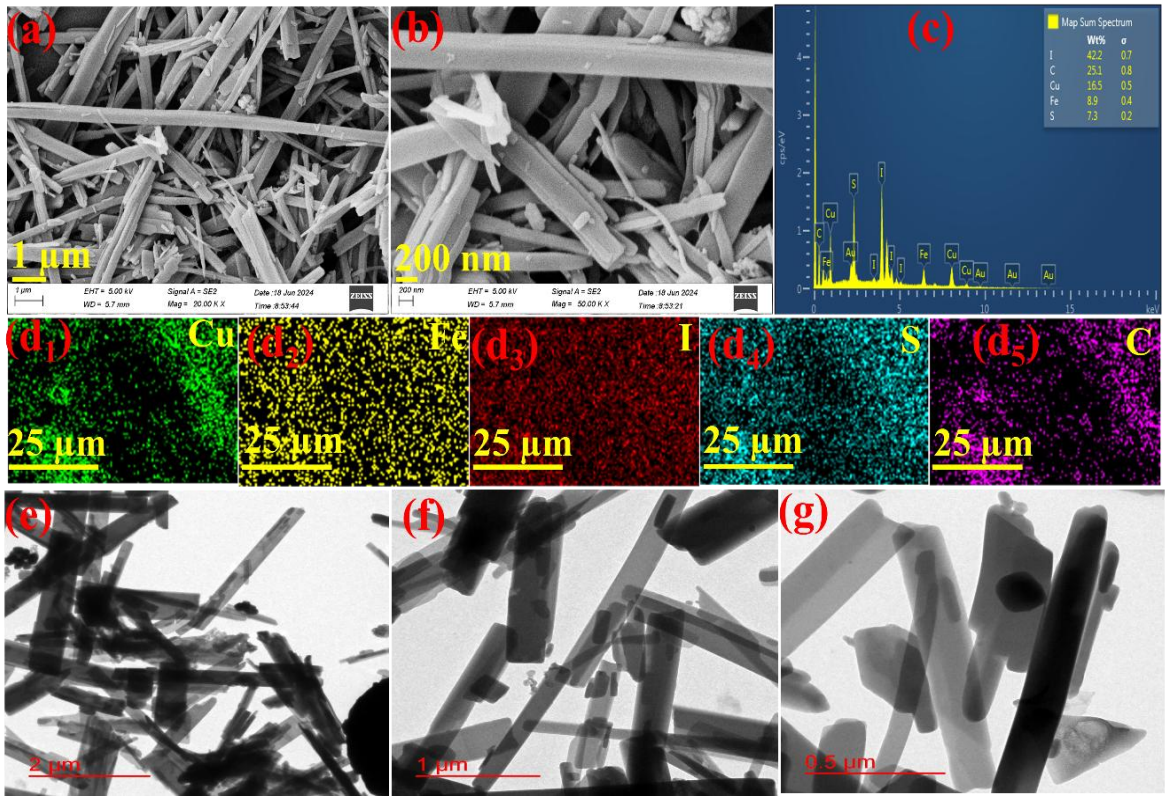


**Figure S14**. Morphological and elemental analysis of **Fc-Cu1**. (a) SEM image at 1 **µ**m (b) SEM image at 200 nm (c) EDS of **Fc-Cu1** ($d_1$-$d_5$) elemental mapping of Cu, Fe, I, S and C, (e) TEM images of **Fc-Cu1** at 2 **µ**m (f) TEM image of **Fc-Cu1** obtained at 1 **µ**m (g) TEM image of **Fc-Cu1** at 0.5 **µ**m

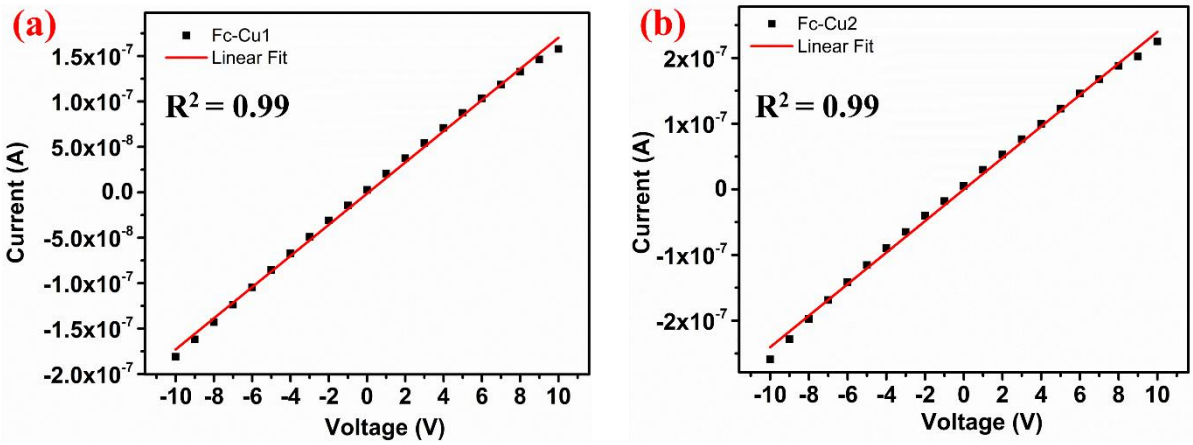


**Figure S15**. Electrical conductivity of (a) **Fc-Cu1** and (b) **Fc-Cu2**

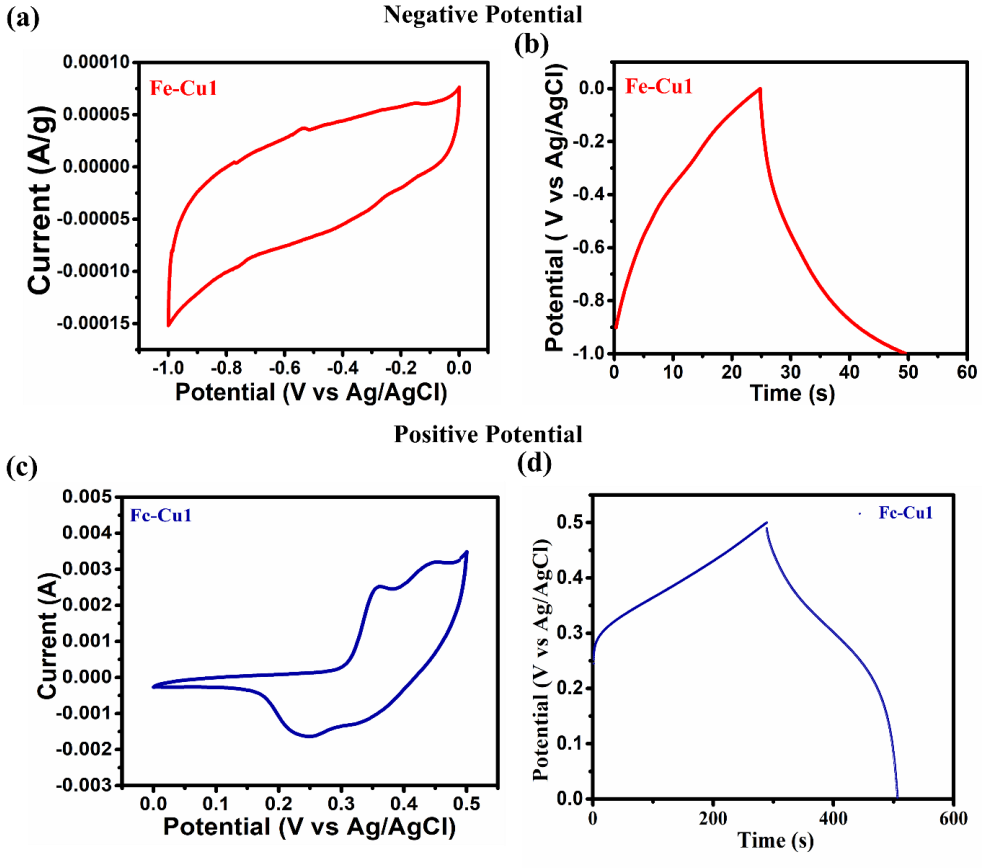


**Figure S16**. (a-b) CV and GCD of **Fc-Cu1** in negative potential at 10 $mVs^{-1}$ and 1 $Ag^{-1,}$ respectively; (c-d) CV and GCD of **Fc-Cu1** in positive potential at 10 $mVs^{-1}$ and 1 $Ag^{-1,}$ respectively.

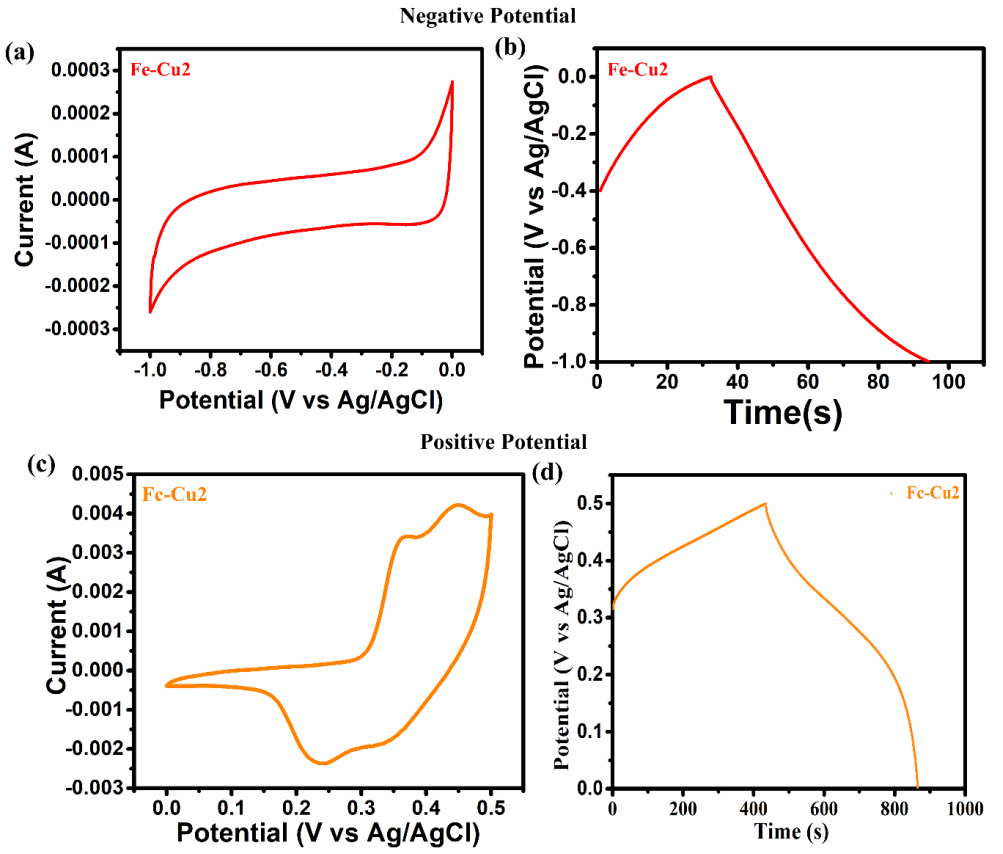


**Figure S17**. (a-b) CV and GCD of **Fc-Cu2** in negative potential at 10 $mVs^{-1}$ and 1 $Ag^{-1,}$ respectively; (c-d) CV and GCD of **Fc-Cu2** in positive potential at 10 $mVs^{-1}$ and 1 $Ag^{-1,}$ respectively.

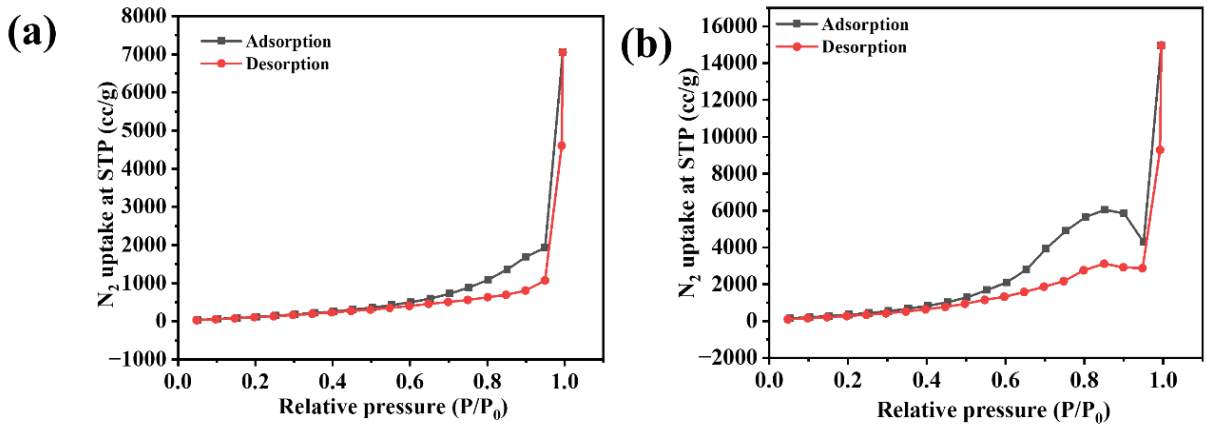


**Figure S18:** BET surface area analysis of (a) **Fc-Cu1** and (b) **Fc-Cu2**.

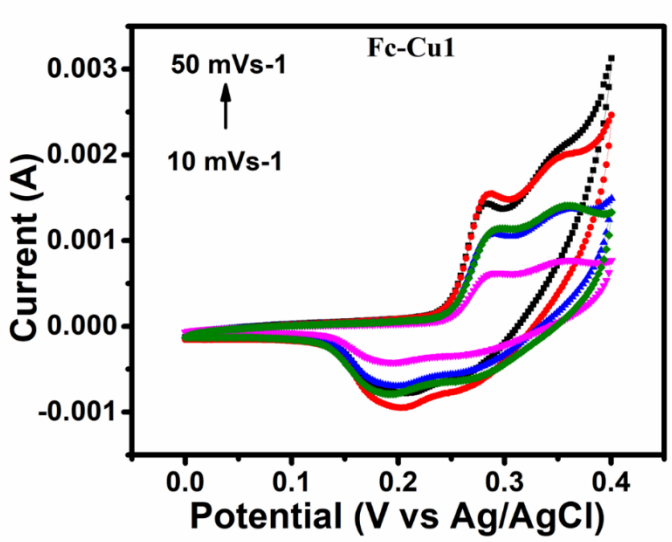


**Figure S19.** CV of **Fc-Cu1** at different scan rates

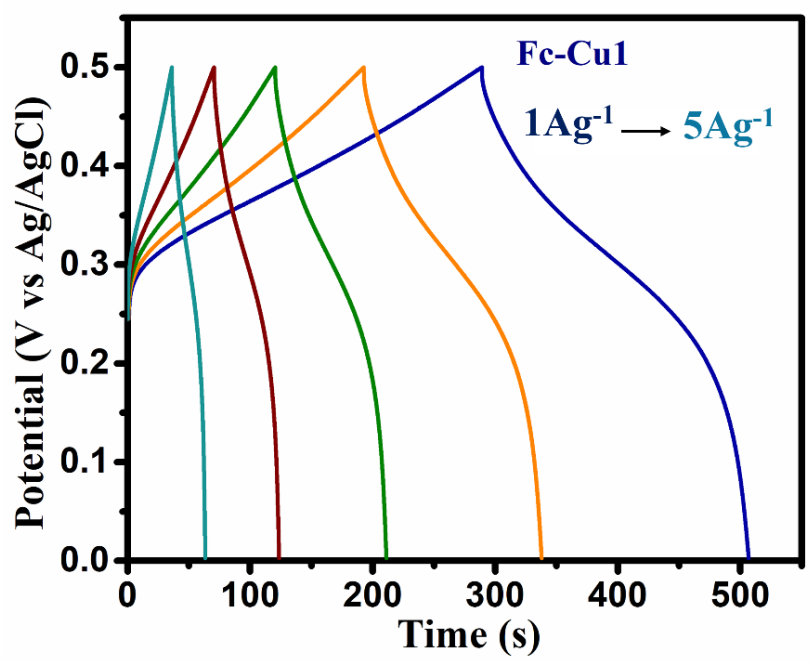


**Figure S20.** GCD at different current densities of **Fc-Cu1**

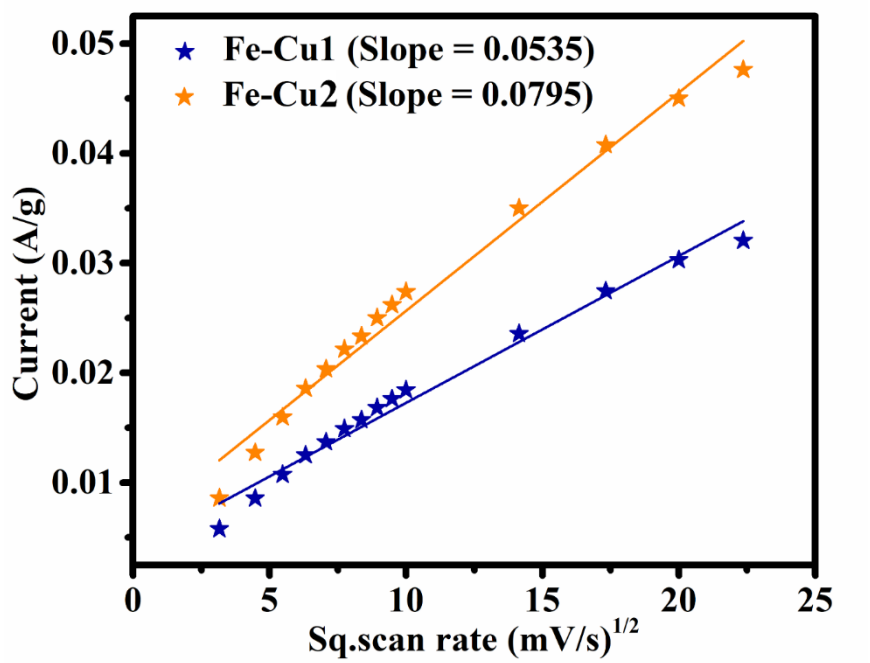


**Figure S21.** Electrochemical kinetics analysis: Peak current (highest current, A) vs. square root of scan rate $(mVs^{-1})^{1/2}$ graph plots of **Fc-Cu1** and **Fc-Cu2** at different scan rates between 10 to 50 $mVs^{-1}$.

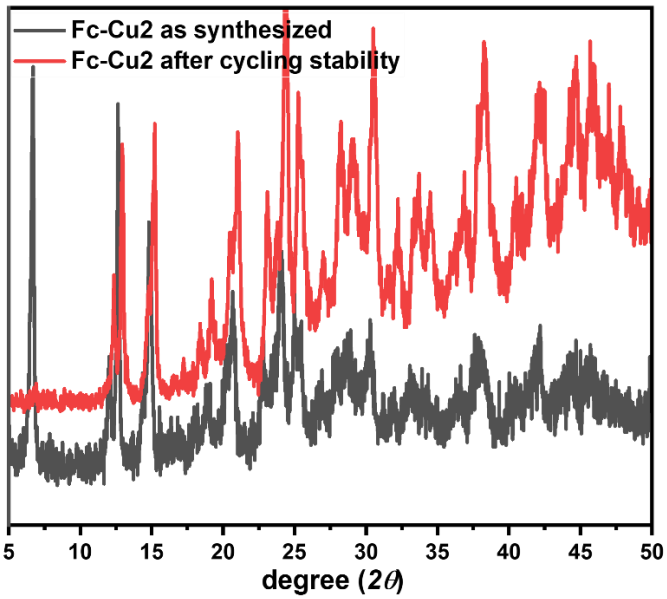


**Figure S22:** Comparison of PXRD patterns of **Fc-Cu2** before and after cycling stability (5000 cycles)

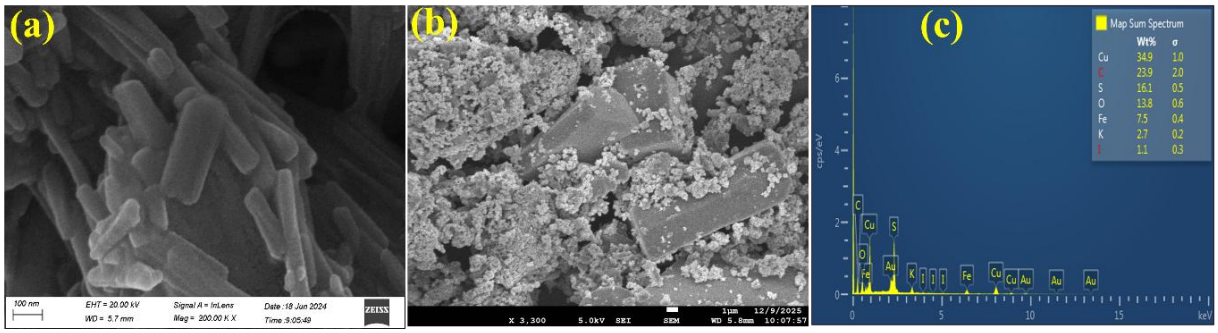


**Figure S23:** FE-SEM image of **Fc-Cu2** (a) as synthesized, (b) after cycling stability test (5000 cycles) (c) EDS spectrum of **Fc-Cu2** after cycling stability

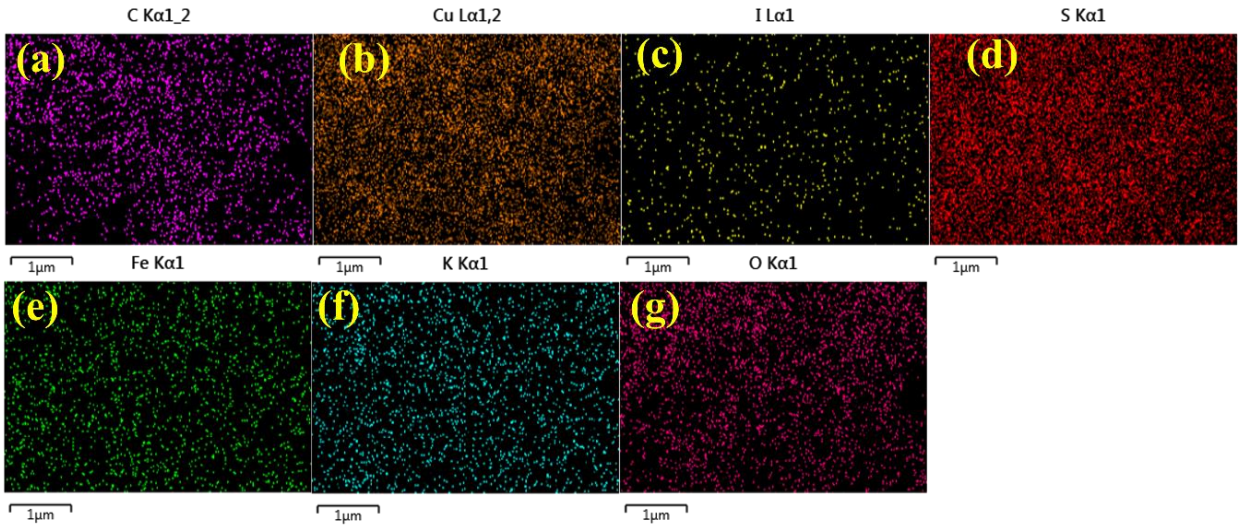


**Figure S24:** Elemental mapping of **Fc-Cu2** after cycling stability

**Table S2.** Comparison table for efficiency in devices.

| **Metal complex** | **Electrolyte** | **$E_d$ (Wh $Kg^{-1}$)** | **$P_d$ (W $Kg^{-1}$)** | **Voltage range (V)** | **Specific capacity /capacitance** | **Cycling stability** | **Ref.** |
|---|---|---|---|---|---|---|---|
| HBCOH-Cu | 1M KCl | 12.11 | 8550 | 0 – 1.5 | 308 F $g^{-1}$ @ 0.2 A $g^{-1}$ | 90%, 5000 cycles | *Angew. Chem. Int. Ed.* **2025**, e202500324 |
| Ni-TTC | 1M KCl | 9.3 | 2430 | 0 – 1.2 | 187 F $g^{-1}$ @ 0.2 A $g^{-1}$ | 54%, 2000 cycles | *Adv. Funct. Mater.* **2023**, 33, 2301513. |
| Cu-MOF | 1M $Na_2SO_4$ | 30.56 | 600 | 0 – 1.2 | 153 F $g^{-1}$ @ 0.5A $g^{-1}$ | 90%, 10000 cycles | *Chem. Eng. J.* **2022**, 435 135042 |
| Co(2,6-NDC) (DPNDI) | 1M LiOH | 22.16 | 6433 | -1.2 –1.2 | 25.5 F $g^{-1}$ @ 1 A $g^{-1}$ | 98%, 30000 cycles | *ACS Materials Lett.* **2025**, 7, 1852−1859 |
| $CuAg_4$(BHT) | 1M KCl | 17.1 | 446.1 | 0 – 1.8 | 38 F $g^{-1}$ @ 0.5 A $g^{-1}$ | 90%, 5000 cycles | *Mater.Horiz.*, **2023**,10, 3821-3829 |
| CuCN-MOF | 6M KOH | 62.9 | 1100 | 0 – 2 | 266.5 C $g^{-1}$ @ 1 A $g^{-1}$ | 81.1%, 5000 cycles | *Inorg. Chem.* **2023**, 62, 11, 4672–4679 |
| PSC2 | 1M $Na_2SO_4$ | 161 | 2416 | -1.2 –1.2 | 455 F $g^{-1}$ @ 3A $g^{-1}$ | 93%, 4000 cycles | *Chem. Eur. J.* ***2020****, 26, 9518 – 9526* |
| (Cu-TBC) | 0.1M $H_2SO_4$ | 18.89 | 6000 | 0 – 0.6 | 377 F $g^{-1}$ @ 0.5 A $g^{-1}$ | 83%, 5000 cycles | *Chem. Commun.*, **2023**,59, 2978-2981 |
| Fe-Tp | 5 M $H_2SO_4$ | 5.31 | ≈1200 | 0 – 1.2 | 122 F $g^{-1}$ @ 0.1 A $g^{-1}$ | 80%, 36000 cycles | *Chem. Eng. J.* **2024**, 496 153589 |
| Cu-DBC | 1M NaCl | 7.6 | 5001 | 0 – 0.8 | 396 F $g^{-1}$ @ 0.1 A $g^{-1}$ | 80%, 2000 cycles | *Angew. Chem. Int. Ed.* ***2020****, 59, 1081.* |
| Cu(I)CN-MOF | 1M KOH | 68.175 | 5540 | 0 – 0.9 | 136.48 $Cg^{-1}$ @ 1A $g^{-1}$ | 96.5%, 10000 cycles | *J. Mater. Chem. A*, **2024**,12, 4534-4543 |
| **Fc-Cu2** | **1M KOH** | **14.5** | **6000** | **0 – 1** | **104 C $g^{-1}$ @ 1 A $g^{-1}$** | **85 %, 10000 cycles** | **This work** |

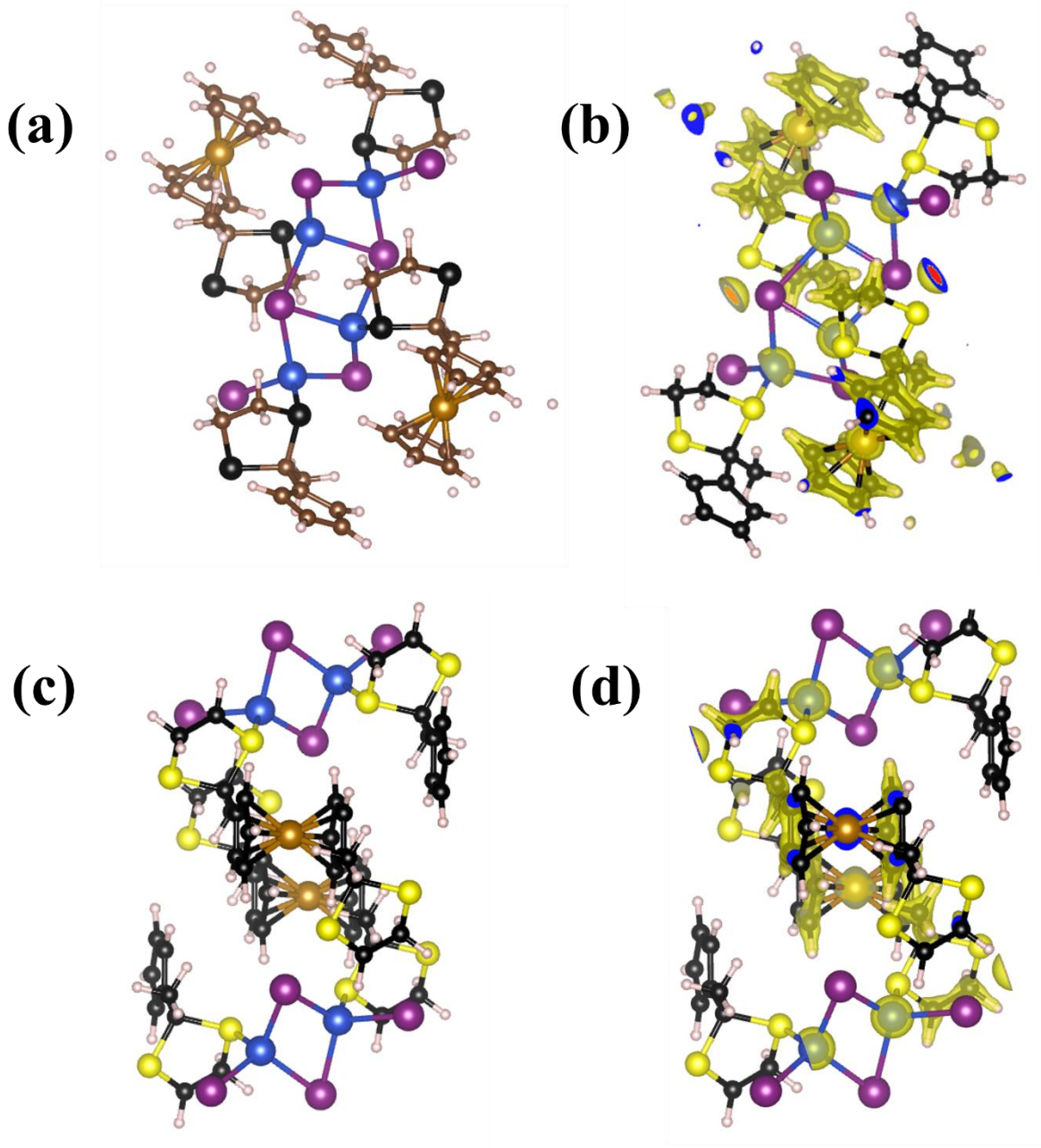


**Figure S25:** Presents the following: (a) The equilibrium structure of the pristine **Fc-Cu1**, (b) The charge density distribution of (c) **Fc-Cu1** framework, in yellow, shows the charge accumulation; (b) The equilibrium structure of the pristine **Fc-Cu2**, (b) The charge density distribution of (c) **Fc-Cu2** framework, in yellow, shows the charge accumulation.

**Table S3: Bader charge density analysis**

| | **Fc-Cu1** | | | **Fc-Cu2** | |
|---|---|---|---|---|---|
| | Monkhorst | | Atoms | Monkhorst | Bader Charge |
| Atoms | Kpoint | Bader Charge | | Kpoint | |
| I | 7.397402 | -0.397402 | I | 7.462605 | -0.462605 |
| I | 7.397384 | -0.397384 | I | 7.462605 | -0.462605 |
| I | 7.463608 | -0.463608 | I | 7.358256 | -0.358256 |
| I | 7.463608 | -0.463608 | I | 7.358256 | -0.358256 |
| Cu | 10.625706 | 0.374294 | Cu | 10.620923 | 0.379077 |
| Cu | 10.625675 | 0.374325 | Cu | 10.620884 | 0.379116 |
| Cu | 10.612923 | 0.387077 | Cu | 10.610667 | 0.389333 |
| Cu | 10.612923 | 0.387077 | Cu | 10.610703 | 0.389297 |
| Fe | 6.941899 | 1.058101 | Fe | 7.024726 | 0.975274 |
| Fe | 6.941899 | 1.058101 | S | 6.02806 | -0.02806 |
| S | 6.010115 | -0.010115 | S | 5.857535 | 0.142465 |
| S | 6.010115 | -0.010115 | S | 5.857535 | 0.142465 |
| S | 6.038895 | -0.038895 | S | 3.935101 | 0.064899 |
| S | 6.038895 | -0.038895 | C | 3.935101 | 0.064899 |
| C | 4.127289 | -0.127289 | C | 4.128431 | -0.128431 |
| C | 4.127289 | -0.127289 | C | 4.128431 | -0.128431 |
| C | 4.185326 | -0.185326 | C | 4.014311 | -0.014311 |
| C | 4.185326 | -0.185326 | C | 4.014311 | -0.014311 |
| C | 4.176946 | -0.176946 | C | 4.098825 | -0.098825 |
| C | 4.176946 | -0.176946 | C | 4.098825 | -0.098825 |
| C | 4.144353 | -0.144353 | C | 4.134923 | -0.134923 |
| C | 4.144353 | -0.144353 | C | 4.134923 | -0.134923 |
| C | 4.133398 | -0.133398 | C | 4.094663 | -0.094663 |
| C | 4.133398 | -0.133398 | C | 4.094672 | -0.094672 |
| C | 4.169894 | -0.169894 | C | 4.097671 | -0.097671 |
| C | 4.169894 | -0.169894 | C | 4.097671 | -0.097671 |
| C | 4.168687 | -0.168687 | C | 4.114666 | -0.114666 |
| C | 4.168687 | -0.168687 | C | 4.114666 | -0.114666 |
| C | 4.175952 | -0.175952 | C | 4.248076 | -0.248076 |

| | | | | | |
|---|---|---|---|---|---|
| C | 4.175952 | -0.175952 | C | 4.248076 | -0.248076 |
| C | 4.196334 | -0.196334 | C | 0.99434 | 0.00566 |
| C | 4.196332 | -0.196332 | C | 0.994339 | 0.005661 |
| C | 4.145905 | -0.145905 | C | 0.988283 | 0.011717 |
| C | 4.145905 | -0.145905 | C | 0.988283 | 0.011717 |
| C | 4.086405 | -0.086405 | C | 0.978392 | 0.021608 |
| C | 4.086405 | -0.086405 | C | 0.978392 | 0.021608 |
| C | 3.998435 | 0.001565 | C | 0.947416 | 0.052584 |
| C | 3.998435 | 0.001565 | C | 0.947416 | 0.052584 |
| C | 4.11067 | -0.11067 | C | 0.948646 | 0.051354 |
| C | 4.11067 | -0.11067 | C | 0.948654 | 0.051346 |
| C | 4.076866 | -0.076866 | C | 0.968771 | 0.031229 |
| C | 4.076866 | -0.076866 | H | 0.968771 | 0.031229 |
| H | 0.924205 | 0.075795 | H | 0.964971 | 0.035029 |
| H | 0.924205 | 0.075795 | H | 0.964971 | 0.035029 |
| H | 0.930702 | 0.069298 | H | 1.004207 | -0.004207 |
| H | 0.930702 | 0.069298 | H | 1.004203 | -0.004203 |
| H | 0.955789 | 0.044211 | H | 0.956953 | 0.043047 |
| H | 0.955786 | 0.044214 | H | 0.956953 | 0.043047 |
| H | 0.939216 | 0.060784 | H | 0.930949 | 0.069051 |
| H | 0.939216 | 0.060784 | H | 0.93093 | 0.06907 |
| H | 0.916346 | 0.083654 | | | |
| H | 0.916346 | 0.083654 | | | |
| H | 0.931153 | 0.068847 | | | |
| H | 0.931145 | 0.068855 | | | |
| H | 0.944859 | 0.055141 | | | |
| H | 0.944859 | 0.055141 | | | |
| H | 0.921963 | 0.078037 | | | |
| H | 0.921965 | 0.078035 | | | |
| H | 0.928294 | 0.071706 | | | |
| H | 0.928294 | 0.071706 | | | |
| H | 0.957166 | 0.042834 | | | |
| H | 0.957166 | 0.042834 | | | |

| | | | |
|---|---|---|---|
| H | 0.993492 | 0.006508 | |
| H | 0.993492 | 0.006508 | |
| H | 0.967935 | 0.032065 | |
| H | 0.967935 | 0.032065 | |
| H | 0.92282 | 0.07718 | |
| H | 0.922822 | 0.077178 | |
| H | 0.918779 | 0.081221 | |
| H | 0.918779 | 0.081221 | |
| H | 0.916813 | 0.083187 | |
| H | 0.91681 | 0.08319 | |
| H | 0.943494 | 0.056506 | |
| H | 0.943494 | 0.056506 | |

**References:**


[1] CrysAlisPro Software System, Oxford Diffraction Ltd., **2010**.

[2] Bruker, *Apex3*, Bruker AXS Inc., Madison, Wisconsin, USA **2018**.

[3] Bruker, *Apex4*, Bruker AXS Inc., Madison, Wisconsin, USA **2021**.

[4] Bruker, *Apex4*, Bruker AXS Inc., Madison, Wisconsin, USA **2023**.

[5] O. V. Dolomanov, L. J. Bourhis, R. J. Gildea, J. A. K. Howard, H. Puschmann, *J. Appl. Cryst.* **2009**, *42*, 339–341.

[6] G. M. Sheldrick, *Acta Cryst.* **2015**, *A71*, 3–8.

[7] G. M. Sheldrick, *Acta Cryst.* **2015**, *C71*, 3–8.